1992

Reduction of Chromium (VI) when Solar Selective Black Chromium is Deposited in the Presence of Organic Additive

Branko N. Popov
University of South Carolina - Columbia, popov@engr.sc.edu

Ralph E. White
University of South Carolina - Columbia, white@cec.sc.edu

D. Slavkov
University Kiril and Metodij, Skopje, Yugoslavia

Z. Koneska
University Kiril and Metodij, Skopje, Yugoslavia

Publication Info

Journal of the Electrochemical Society, 1992, pages 91-98.

DOI: 10.1149/1.2069206
http://dx.doi.org/10.1149/1.2069206

14. L. T. Romankiw, S. Krongelb, E. E. Castellani, A. T. Pfeiffer, B. J. Stoeber, and J. D. Olsen, *IEEE Trans. Mag.*, **MAG-10,** 828 (1974).
15. D. A. Rudy, Abstract 264, p. 658, The Electrochemical Society Extended Abstracts, Vol. 76-1, Washington, DC, May 2-7, 1976.
16. D. A. Rudy, Abstract 266, p. 685, The Electrochemical Society Extended Abstracts, Vol. 76-2, Las Vegas, NV, Oct. 17-22, 1976.
17. B. Littwin, *IEEE Trans. Mag.*, **MAG-14,** 123 (1978).
18. J. Horkans and L. T. Romankiw, *This Journal,* **124,** 1499 (1977).
19. J. Dukovic, *IBM J. Res. Develop.*, **34,** 693 (1990).
20. R. C. Alkire, T. Bergh, and R. L. Sani, *This Journal,* **125,** 1981 (1978).
21. R. C. Alkire and D. B. Reiser, *Electrochim. Acta,* **28,** 1309 (1983).
22. E. C. Hume, III, W. M. Deen, and R. A. Brown, *This Journal,* **131,** 1251 (1984).
23. U. Landau, R. T. Galasco, and J. Tang, Abstract 330, p. 484, The Electrochemical Society Extended Abstracts, Vol. 88-2, Chicago, IL, Oct. 9-14, 1988.
24. T. Kessler and R. C. Alkire, *Plat. Surf. Finish.*, **63,** 22 (1980).
25. S. Mehdizadeh, J. Dukovic, P. C. Andricacos, L. T. Romankiw, and H. Y. Cheh, *This Journal,* **137,** 110 (1990).
26. A. T. Kuhn, "Techniques in Electrochemistry, Corrosion and Metal Finishing—A Handbook," pp. 95-116, John Wiley & Sons, Inc., New York (1987).
27. N. Ibl, "Comprehensive Treatise of Electrochemistry," Vol. 6, Plenum Publ. Corp., New York (1982).
28. C. A. Brebbia and S. Walker, "Boundary Element Techniques in Engineering," Newnes-Butterworths, Boston (1980).
29. J. Dukovic and C. W. Tobias, *This Journal,* **134,** 331 (1987).
30. L. Lapidus, "Digital Computation For Chemical Engineers," p. 227, McGraw Hill, Inc., New York (1962).
31. M. Matlosz, C. Creton, C. Clerc, and D. Landolt, *This Journal,* **134,** 3015 (1987).
32. M. Datta and L. T. Romankiw, *ibid.*, **136,** 285C (1989).

Reduction of Chromium (VI) when Solar Selective Black Chromium is Deposited in the Presence of Organic Additive

B. N. Popov* and R. E. White*

Department of Chemical Engineering, Texas A&M University, College Station, Texas 77843-3122

D. Slavkov and Z. Koneska

Faculty of Technology and Metallurgy, University "Kiril and Metodij," Skopje, 91000, Yugoslavia

ABSTRACT

Electrochemical dc methods were used to study the reduction of chromium (VI) in the presence of organic additives. It is shown that F^-, thiourea, and citric acid are essential to enable deposition of black chrome from concentrated chromic acid solutions. A new formulation of the plating bath is defined. The optimum operating conditions under which spectrally selective surface of black chrome is deposited have been determined.

The classical process of chromium deposition begins simultaneously with formation of the oxide layer which rapidly deteriorates permitting the access of Cr(VI) ions to the cathode and their reduction to metallic chromium. According to the polarization studies (1-10), the cathodic oxide film is formed only if a polychromate ion exists in the electrolyte. Polychromates are formed in strong solutions of chromic acid at low pH. The sulfate ion present in conventional chroming bath exists in strong acids as HSO_4^- and favors the elimination of the cathodic oxide film (11). A phenomenological model for the deposition of Cr from hexavalent baths was proposed by Hoare *et al.* (7-10). According to these authors the polychromates decompose to chromous hydroxide and a dichromate which can polymerize back to a trichromate by condensation with other chromates in the solution. The HSO_4^-, exerts its catalytic activity by forming a chromousoxybisulfate complex through hydrogen bonding with chromous oxide. With the successive transfer of two electrons to the specifically absorbed chromousoxybisulfate complex on the cathode surface, Cr(I) and finally metallic Cr along with the regenerated HSO_4^- ion are then obtained.

According to Saiddington and Hoey (12), reduction of pure chromic acid in the absence of sulfate ions results in formation of an amorphous oxide film which grows on the cathode. This film prevents the metal reduction processes from taking place on the cathode surface, while allowing the reduction of hydrogen only. The existence of such films has been proved by double layer capacity measurements (13) and optical microscope studies (14).

* Electrochemical Society Active Member.

The deposition of black chromium is generally done with conventional chroming bath free from sulfates, to which catalyst such as acetic acid, sodium nitrate, ammonium methavanadate or fluorine compounds are added (15-21). The exact mechanism by which the catalyst ions enable chromium reduction which leads to formation of black deposits is still open to conjecture.

One of the most common commercial solutions for black chrome deposition is ChromOnyx plating solution from the Harshaw Chemical Co., which contains acetic acid as catalyst. As reported in the literature (17), use of this solution may lead to production of black chrome surfaces with different optical properties as a result of the degradation process of the catalyst. The purpose of the present work is to study the electrochemical reduction of chromic acid in the presence of organic additives and to determine the electroplating conditions for obtaining a selective absorbing surface. An attempt has been made to define a new formulation of plating bath containing NaF, citric acid, and thiourea. The preliminary polarization studies have shown that these compounds are essential to enable deposition of black chromium.

Experimental

In order to establish the influence of the constituents of the plating on the reduction of chromic acid, measurements of the rest potential at open circuit and c.v. measurements were made. All electrochemical measurements were carried out in a special Teflon cell because of the presence of fluorine ions. Working Pt electrodes were used, mounted into a Teflon holder with a geometric area of 6.2×10^{-3} cm^2. The electrodes were mechanically pol-

ished, ultrasonically cleaned in an alcohol and rinsed with distilled water prior to each measurement. A standard calomel electrode (SCE) was used as a reference electrode. Black chrome was electrodeposited from a solution containing 4*M* CrO_3 and 0.05*M* $BaCO_3$ in presence of fluorine ions and organic additives. The additives were added in the cathode compartment during the course of the run.

All electrochemical measurements were carried out using a PAR Model 273 potentiostat-galvanostat connected via Model 273 interface, to an IBM computer. Experimental data were stored and plotted using a 7470 Hewlett-Packard plotter.

An ideal selective surface is totally reflecting, or white to the infrared radiation emitted by a black body at the temperature of operation of the collector. However, an ideal selective surface does not exist in practice, and therefore one can conceive a real surface whose spectral reflection coefficient varies with wavelength in a manner close to that of an ideal black body. Such a surface can be characterized by its hemispherical absorptance, $\mathbf{a}_S$, and its normal thermal emittance, $\mathbf{e}_T$.

Normal reflection spectra of the samples were measured on the Perkin-Elmer Model 180 spectrophotometer equipped with reflection cells. A gold mirror was used as reference for reflection in order to measure the reflectivity of the samples. The measured spectral range was from 2.5 to 50 μm. The reflection spectra of the samples in the range between 0.4 and 2.5 μm have been measured with an Opton II instrument equipped with an integrating sphere for measuring the hemispherical reflectivity. A computer program was used for calculation of the normal thermal emittance ($\mathbf{e}_T$) and the hemispherical absorptance ($\mathbf{a}_S$) from specular normal and hemispherical reflectivities according to the equations

$$e_T = \frac{\int_{0.3\ \mu m}^{\lambda_c} \epsilon(\lambda, T) M^o(\lambda, T) d\lambda}{\int_{0.3\ \mu m}^{\lambda_c} M^o(\lambda, T) d\lambda} \quad [1]$$

and

$$a_S = \frac{\int_{\lambda_c}^{50\ \mu m} \alpha(\lambda, T) E^S(\lambda) d\lambda}{\int_{\lambda_c}^{50\ \mu m} E^S(\lambda) d\lambda} \quad [2]$$

where $\alpha(\lambda, T)$ and $\epsilon(\lambda, T)$ are, the hemispherical spectral absorptance and emittance, respectively, $E^S(\lambda)$ the spectral solar irradiance, and $M^o(\lambda, T)$ the spectral emittance of the black body at temperature T. For opaque materials (transmittance $\tau = 0$) to which black chrome deposits belong, spectral absorptance for directional incidence and the directional emittance can be calculated from the spectral reflectance or directional irradiation as: $\mathbf{a}_S = \epsilon = 1 - \mathbf{r}$, where $\mathbf{r}$ is the spectral reflectance.

Results and Discussion

Open-circuit potential studies.—Open-circuit potentials observed on Pt cathodes in pure chromic acid and in chromic acid in which NaF and organic compounds were added are listed in Table I. High anodic values of the observed open-circuit potentials indicate that platinum passivates spontaneously in oxygen free chromic acid solutions. The rest potentials are probably mixed potentials of the reduction of dichromate ion and oxidation of Pt to PtO (22-29). The passive film is reducing when the cathode is polarized at more negative potentials.

Potentiodynamic measurements.—Potentiodynamic polarization experiments were carried out in order to determine the shape of the cathodic and anodic curves and the existence of the passivation currents. The electroactive Cr species were reduced in a nitrogen atmosphere using Pt working electrodes.

Typical cathodic potentiodynamic polarization curves for electroreduction of pure chromic acid obtained starting at open-circuit potential for different aging times (0.5, 30, 60, and 90 min) are shown in Fig. 1. All curves were

Table I. Open-circuit potential values with respect to (SCE) obtained on platinum electrodes in chromic acid and in solutions catalyzed by F^- ions, thiourea, and citric acid.

Solution	Concentration (*M*)	*E*, (V), (SCE)
$[Cr_3O_{10}]^=$	2.0	0.701
	2.5	0.74
	3.0	0.74
	4.0	0.91
4*M* $[Cr_3O_{10}]^=$ + citric acid	0.15	0.92
	0.45	0.95
	0.80	0.96
	0.12	0.98
4*M* $[Cr_3O_{10}]^=$ + NaF	0.024	1.043
	0.078	1.025
	0.261	1.010
	0.357	1.015
4*M* $[Cr_3O_{10}]^=$ + thiourea	0.25	1.025
	0.48	1.015
	0.60	1.040
	1.1	1.035

obtained using a scan rate of 1 mV/s by scanning from +1.3 V *vs.* SCE to −1.2 V *vs.* SCE. There is no evidence for any differences in the shape of the polarization curves obtained for different waiting times indicating that concentrated chromic acid solution is highly oxidizing and that the passive film formation on the electrode surface is a very fast process. The passive film actually is formed in the first contact of the electrode surface with chromic acid solution. The dichromate ion present in the concentrated chromic acid solution (23-26) is reduced on the surface, oxidizing Pt to PtO. The curves in Fig. 1 also show a decay of the current at +1.0 V *vs.* SCE which indicates a passivation process, while the fine structure of the polarization curves is connected with the passivation process and the changes of the oxidation states of Pt and Cr present in the composition of the passive film. A low hydrogen overvoltage is present on the electrode. According to the observations during the run of the experiment as well as from the curves in Fig. 1, hydrogen evolution starts at −0.25 V *vs.* SCE. Thus, the entire cathodic current corresponds to combination of hydrogen reduction and reduction of Cr ions which occurs at approximately −0.9 V *vs.* SCE (a broad peak in Fig. 1 is observed at this potential).

Figure 2 show potentiodynamic polarization curves taken at sweep rate of 1 mV/s in the presence of 0.2*M* NaF (curve 1), in the presence of 0.35*M* thiourea (curve 2), and in the presence of 0.5*M* citric acid (curve 3). It was found that in the presence of the additives the hydrogen evolution drops drastically and two more cathodic peaks appear at

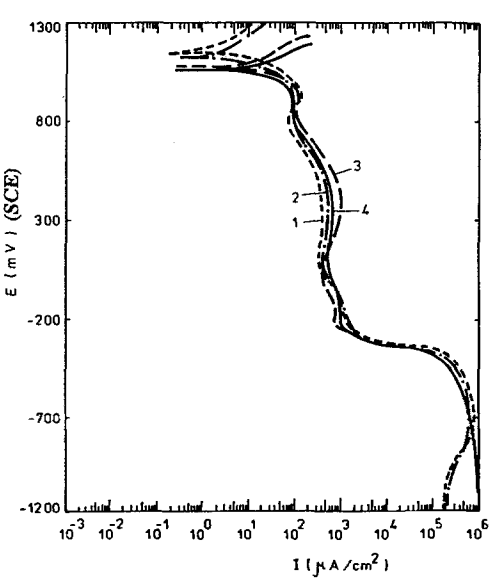

Fig. 1. Typical potentiodynamic polarization curves for electroreduction of 4*M* chromic acid obtained using a scan rate of 1 mV/s and for different aging times: 1, 0.5; 2, 30; 3, 60; and 4, 90 min.

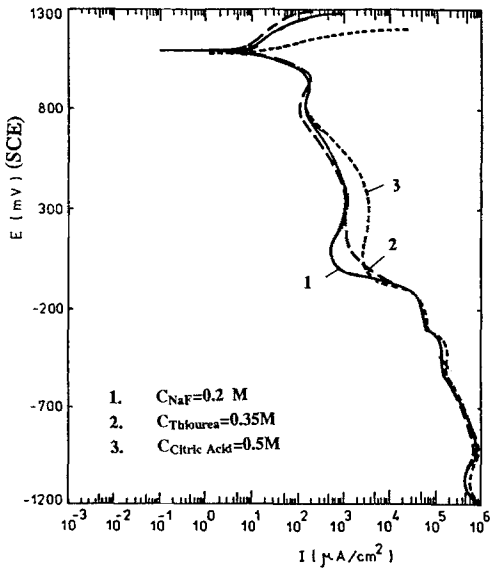

Fig. 2. Potentiodynamic polarization curves for electroreduction of 4M chromic acid obtained in the presence of NaF, thiourea, and citric acid taken at sweep rate of 1 mV/s.

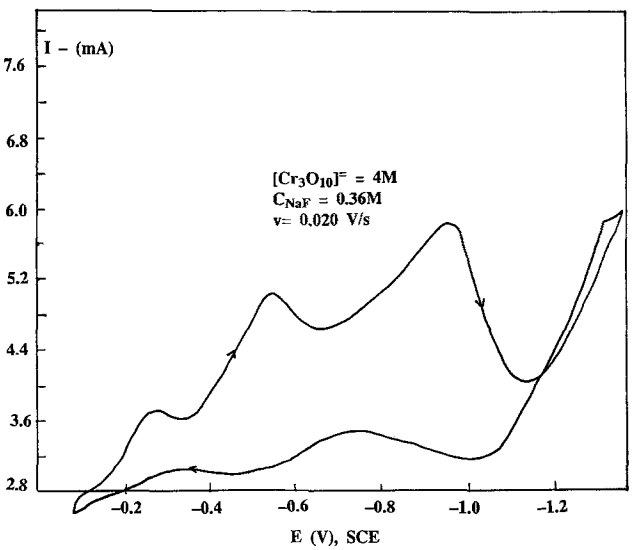

Fig. 4. Cyclic voltammogram for reduction of 4M chromic acid in the presence of 0.36M fluorine ions, v = 0.02 V/s.

-0.3 V and at -0.5 V *vs.* SCE which were studied in more details using cyclic voltammetry.

Cyclic voltammetry.—The curves were obtained using different scan rates in the range from 0.01 V/s up to 0.1 V/s and scanning from -0.2 V *vs.* SCE to -1.2 V *vs.* SCE where the reduction of water becomes a predominant reaction. Figure 3 shows typical c.v. curves for reduction of pure chromic acid (4*M*) in which only 0.05*M* $BaCO_3$ was added in order to precipitate SO_4^{2-} ions. As can be seen from Fig. 3, the curve shows a cathodic maximum at -0.95 V *vs.* SCE which is formed during cathodic course of the run, and this can be attributed to the reduction of Cr ions. There is no evidence of a corresponding anodic peak during the anodic course of the run, indicating that the product formed on the cathode cannot be dissolved when the electrode is polarized anodically. Repeated cycles (curve 2) on the same figure do not show the cathodic peak at -0.95 V, only hydrogen evolution, which indicates that the electrode becomes completely passive during the anodic course of the previous cycle. Neither fluorine, thiourea, nor citric acid have an influence on the magnitude of the reduction peak at -0.95 V, and the peak current only increases with increasing the sweep rate. The peak current was not found to be a linear function of the square root of the sweep rate, suggesting that the process is not diffusion controlled.

Figure 4 shows the cyclic voltammograms for the electrochemical reduction of chromic acid in the presence of 0.36*M* fluorine ions. In the presence of the catalyst ions two more cathodic peaks appear at -0.3 V and at -0.5 V *vs.* SCE. The dependence of the magnitude of the first peak on the concentration of fluorine ions (from 0.33*M* to 0.76*M*) is shown in Fig. 5. The curves were obtained using a scan rate of 0.01 V/s and scanning from 0.0 V to -0.4 V *vs.* SCE. It was found that the magnitude of the peak at -0.3 V does not depend on NaF concentration. This peak appears only at concentrations of the additive higher than 0.31*M* at which the evolution of hydrogen drops drastically.

The peak height of the reduction process at -0.5 V *vs.* SCE depends on the concentration of NaF, Fig. 6. The dependence of the peak currents on the sweep rates (0.005 to 0.050 V/s) for the reduction processes at -0.5 V and at -0.95 V *vs.* SCE is shown in Fig. 7. The curves were obtained in the presence of 0.276*M* NaF and scanning from 0.0 V to -1.2 V *vs.* SCE. The dependence of the peak cur-

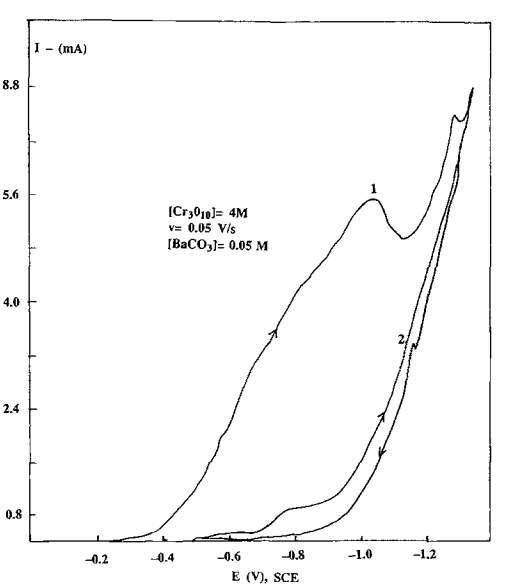

Fig. 3. Cyclic voltammogrrams for reduction of 4M chromic acid, v = 0.050 V/s; 1, first cycle, 2, second cycle.

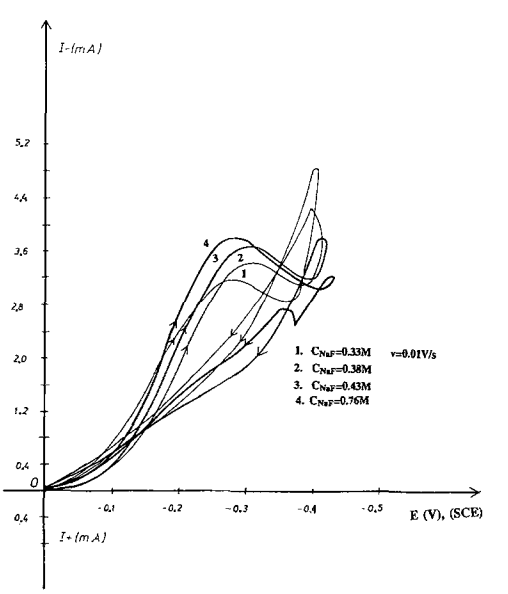

Fig. 5. Cyclic voltammograms for electrochemical reduction of 4M chromic acid at -0.3 V *vs.* SCE, obtained in the presence of different concentrations of NaF, and v = 0.01 V/s.

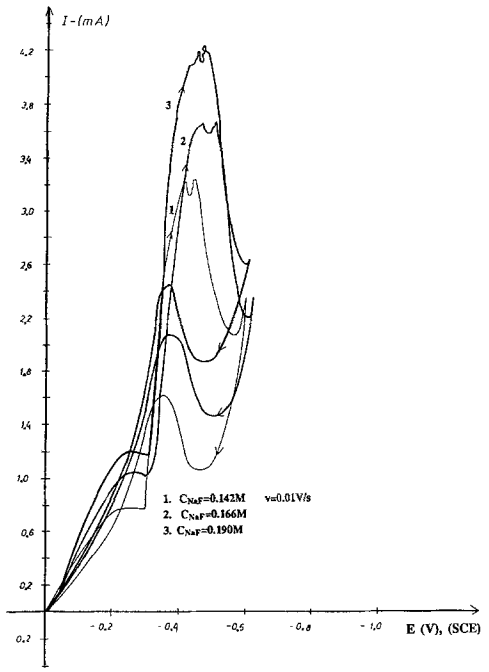

Fig. 6. Cyclic voltammograms for electrochemical reduction of 4M chromic acid at −0.5 V *vs.* SCE, obtained in the presence of different concentrations of NaF, and v = 0.01 V/s.

rent at −0.5 V *vs.* SCE on the square root of the sweep rate is not linear precluding the possibility that the process is diffusion controlled. The reduction, rather, is a surface reaction catalyzed in the presence of F^- ions.

The results obtained for the reduction of chromic acid in the presence of thiourea are similar to those obtained when the reduction was studied in the presence of NaF. The dependence of the magnitude of the peak at −0.3 V on the concentration of thiourea (from 0.23 to 0.38*M*) is shown in Fig. 8. The curves were obtained using a scan rate of 0.02 V/s and scanning from 0.0 V to −0.4 V *vs.* SCE. It was found that the magnitude of the peak does not depend on

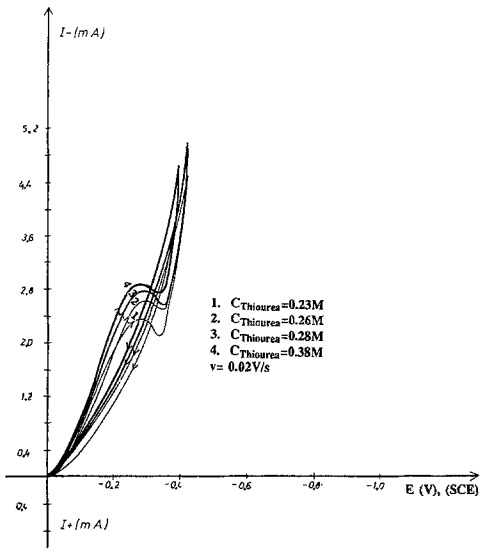

Fig. 8. Cyclic voltammogram for electrochemical reduction of 4M chromic acid at −0.3 V *vs.* SCE, obtained in the presence of different concentrations of thiourea, and v = 0.02 V/s.

thiourea concentration. This peak only appears at concentrations higher than 0.23*M*.

The peak current at −0.5 V depends on the concentration of thiourea, as shown in Fig. 9, but the dependence was not found to be a linear function of the concentration of the additive. The dependence of the peak currents of the reduction processes at −0.5 V and at −0.95 V *vs.* SCE on the sweep rates (0.005 to 0.050) is shown in Fig. 10. The curves were obtained in the presence of 0.2*M* thiourea and scanning from 0.0 V to −1.2 V *vs.* SCE. The peak current at −0.5 V *vs.* SCE was not found to increase with increasing the sweep rate. This suggests that the reduction at −0.5 V in the presence of thiourea is not diffusion controlled.

In Table II are shown cathodic charges (C/cm^2) calculated by integrating the surfaces under the cathodic peaks at −0.5 V in the presence of fluorine ions and thiourea. In the case of NaF additions the charges increase from 10.07×10^{-3} to 95.22×10^{-3} C/cm^2. It is obvious from Table II that both additives have an accentuated influence on the magnitude of the reduction peak at −0.5 V *vs.* SCE, decreasing remarkably the hydrogen evolution.

The potentiodynamic and c.v. measurements as well as the measurements carried out at open circuit indicate that

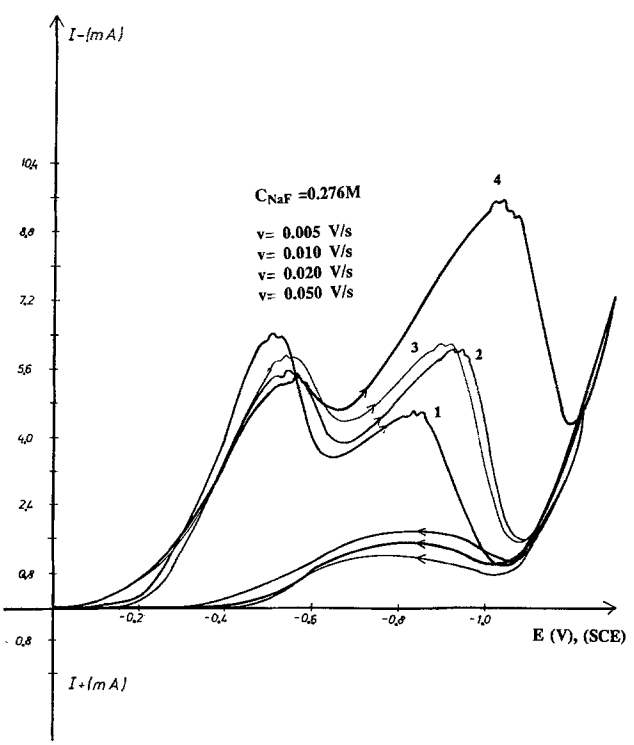

Fig. 7. Cyclic voltammograms for reduction of 4M chromic acid taken for different sweep rates in the presence of 0.276M NaF.

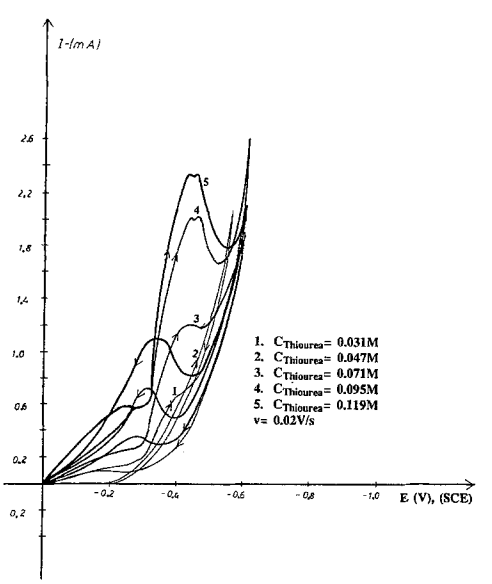

Fig. 9. Cyclic voltammograms for electrochemical reduction of 4M chromic acid at −0.5 V *vs.* SCE, obtained in the presence of different concentrations of NaF, and v = 0.02 V/s.

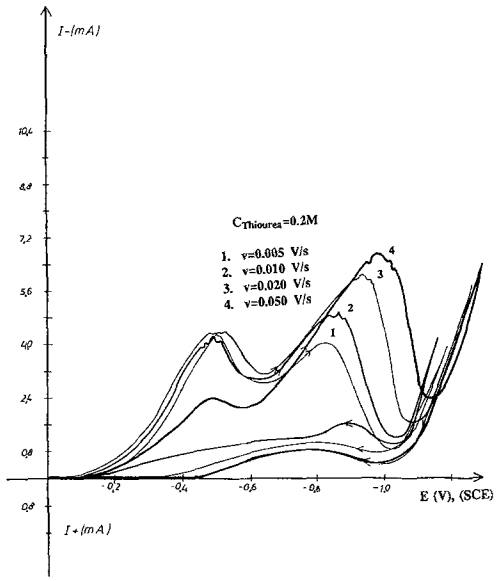

Fig. 10. Cyclic voltammograms for reduction of 4M chromic acid in the presence of 0.2M thiourea taken for different sweep rates.

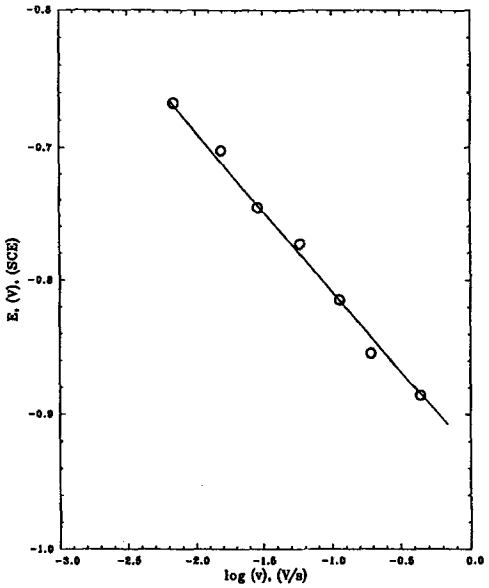

Fig. 11. The shift of the peak potential as a function of log (v).

the passive film formed in concentrated chromic acid has an important role in the reduction mechanism because it shifts the deposition of metallic chromium and chromium oxide to very high overpotentials. Platinum oxides and chromium oxides present in the composition in the film are reduced when the cathode is polarized at −0.35 V *vs.* SCE. As is shown in our polarization studies this process is clearly seen only in the presence of the additives, when the evolution of hydrogen drops drastically. The magnitude of the peak does not depend upon chromic acid concentration or the concentration of the additives indicating that the reduction is not controlled by the ions from the electrolyte.

At further cathodic polarization, a cathodic film is formed, composed from absorbed Cr(VI), Cr(III), and species with lower oxidation states of chromium (30-34).

For any cation which forms complexes in the solution, in order to be reduced or oxidized, it is necessary that its coordination number be changed (22, 24). This fact, in connection with Frank-Condon principle, prevents three-electron reduction from Cr(VI) to Cr(III), because their coordination numbers are 4 and 6, respectively. The reduction of Cr(III) to Cr(II) is also limited, despite that both species have the same coordination number. This limitation results from the structural configuration of the Cr(III) complexes, which are octahedral, while Cr(II) complexes have strong Jahn-Teller distortion of octahedral configuration. Thus, the slow change in the coordination structure compared with the fast electron transfer limits certain electron exchange reactions. Accordingly, the reduction of Cr(VI) to Cr(III) is eliminated as a possibility occurring in one reduction step, rather the reduction occurs through Cr(V) and Cr(IV) intermediaries, where the coordination changes are smaller. According to our studies the peak which occurs at −0.5 V *vs.* SCE can be attributed to reduction of Cr(VI) to Cr(IV). The peak height at −0.5 V *vs.* SCE depends upon the concentration of NaF and thiourea, and, as will be shown later, are essential to enable deposition of black chromium. Cr(VI) ions in concentrated chromic acid solutions essentially are in the form of $Cr_2O_7^{=}$ and in its derivative complexes (7-10, 25-29). The additives used in this study also form complexes with Cr ions. These complexes move toward the cathode through the cathodic film and are reduced at the surface which results in the dependence of the peak height of the reduction process at −0.5 V *vs.* SCE upon the concentration of the additives. Thus, the complexes formed in the cathode region catalyze the transient stages in the electrodeposition process.

Table II. Cathodic charges calculated in integrating the surfaces under the peaks at −0.5 V (SCE) as a function of the concentration of NaF and thiourea.

Solution	Q (C/cm^2) × 10^{-3}
4*M* $[Cr_3O_{10}]^{=}$ + NaF (*M*)	
0.024	10.07
0.048	15.89
0.072	23.12
0.096	40.15
0.110	47.69
0.144	70.35
0.168	88.93
0.192	95.22
4*M* $[Cr_3O_{10}]^{=}$ + thiourea (*M*)	
0.25	15.40
0.48	20.35
0.55	35.68
0.85	47.12
1.10	59.65

The important features of the diagrams in Fig. 7 and Fig. 10 are the increase of the peak current and the shift of the peak-potential with an increase of the sweep rate. This shift of the peak potential with the increased sweep rate is plotted in Fig. 11 as a function of log v as suggested by Srinivasan and Gileadi for the case when the product of the electrochemical reaction are absorbed species which block the surface for further reaction. As seen, a linear dependence is obtained. According to Srinivasan and Gileadi (35), the peak potential and sweep rate [v, V/s], should be related by equation

$$E_p = \frac{RT}{\alpha F} \ln \frac{kF}{k_1 RT} + \frac{RT}{\alpha F} \ln v \qquad [3]$$

where α is the transfer coefficient, k_1 is the reaction rate constant, and k is the amount of charge required to form a monolayer of absorbed product. The linearity obtained in Fig. 11 which follows the prediction of Eq. [3] indicates that the peak at −0.95 V probably results from Cr(IV) to Cr(III) reduction on the surface of the electrode. The product of the electrochemical reduction at this potential are Cr(III) species which form stable electrochemically nonactive complexes with F^- and very stable $[Cr(H_2O)_6]^{3+}$, also an electrochemically nonactive complex in water solutions. These complexes are absorbed at the electrode blocking the surface for further reduction. From the slope in Fig. 11 one can calculate $\alpha = 0.6$. At more cathodic potential, reduction to metallic chromium also occurs with heavy hydrogen evolution as a result of water reduction at high overvoltages.

The amount of liberated hydrogen during the electrodeposition of black chromium from chromic acid solution in

Table III. Hydrogen evolution as a function of the applied potential, $A_{Pt} = 0.6$ cm^2.

−E (V) (SCE)	Hydrogen evolution (H.E.) in 4M citric acid (ml)	H. E. in catalyzed chromic acid with 0.238M F^- (ml)	H. E. in catalyzed 4M chromic acid solution with 0.48M thiourea (ml)
0.293	—	—	—
0.416	4.0	1.4	1.8
0.509	8.15	3.05	5.6
0.866	32.75	4.15	6.4
0.932	40.60	5.00	6.9
1.028	58.40	6.30	8.2
1.040	75.35	7.80	9.9
1.203	over 100	8.30	14.8
1.360	—	13.7	—

the absence and in the presence of the additives was measured quantitatively and the results are given in Table III. The experiments were carried out in a special hermetically sealed cell with an outlet connected to a device where hydrogen gas was collected and its volume measured during the run of the experiment. As seen from Table III the hydrogen evolution drops drastically in the presence of the additives.

Electrodeposition of black chromium.—Optical microscope investigations were carried out in order to analyze the reduction products at −0.3, −0.5, and −0.95 V *vs.* SCE. No evidence was found that any type of deposit is formed on the Pt surface when chromic acid was potentiostatically electrolyzed at −0.3 and at −0.5 V. Evidence of black chrome deposits on the Pt surface was found only in the case when the electrode was polarized at potentials more negative than −0.95 V and in the presence of NaF concentrations higher than 0.3*M*. The amount of the deposited material increases with the increase of the concentration of the catalyst in the electrolyte up to 0.5*M*, when it levels off. Further increase in the fluorine ion concentration inhibits the deposition process. In the absence of fluorine ions in the electrolyte, only dark grayish deposits were obtained, indicating that catalyst ions are essential for the process which leads to a formation of black chrome deposits.

In order to determine the optimum operating conditions under which a spectrally selective surface of black chrome appears, spectral reflectance of black chrome deposited on nickel-plated copper has been studied as a function of deposition time. The following standard experimental conditions were used in preparing the samples for reflectance measurements: agitation of the electrolyte with nitrogen, temperature 295°K, current density 10-12 A/dm^2, cathode to anode area ratio 1:1. A computer program was used to calculate the normal thermal emittance and the hemispherical absorptance from specular normal and hemispherical reflectivities in order to determine the selective properties of the electroplated black chrome coatings. Figure 12 shows reflection spectra of two black chrome deposits in a "as prepared" state electrolyzed for 60 s (curve 1) and for 120 s (curve 2). Variation of the optical properties of these two black chrome specimens are given in Table IV. The data indicate that specimen 1 has better optical characteristics, which can be explained by the influence of the thickness on the optical properties of the deposit.

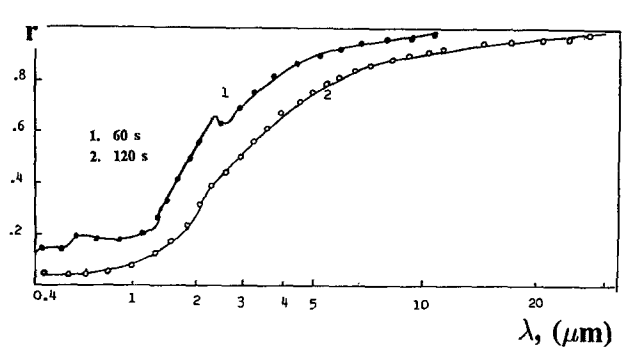

Fig. 12. Spectral reflection spectra of two black chrome deposits prepared onto nickel plated copper at 0.5 A/cm^2 for 1 min (curve 1) and for 2 min (curve 2).

Table IV. Variation of the normal thermal emittance (e_T), the hemispherical absorptance (a_S) and selectivity (a_S/e_T) of black chromium deposited for 1 min (curve 1) and for 2 min (curve 2).

Optical properties	Deposited for 1 min	Deposited for 2 min
a_S	0.916	0.928
e_T (40°C)	0.039	0.100
a_S/e_T (40°C)	23.490	9.280
e_T (200°C)	0.100	0.167
a_S/e_T	9.160	5.650

On the basis of these preliminary measurements we have formulated our own composition of chromate bath, which was used for electrodeposition of black chrome. The best results concerning black chrome deposition were obtained with a bath, whose composition is given in Table V. The tests were carried out on steel samples previously nickel-plated by electrolysis in a Watts bath and on copper samples previously also coated with nickel. The thickness of the nickel coating was about 20 μm in the case when steel samples were used and about 10 μm when copper samples were used. The optimum thermo-optical properties were obtained within 60 s. The optimum plating parameters proved to be current density of 0.35 A/cm^2 and a solution temperature of 18°C. Using the above we obtained black chromium coatings with "**a**" values of 0.94 and "**e**" values of 0.07-0.12. Both thermo-optical properties of the black chromium coating were found to depend upon the deposition time, but they were independent of the type of nickel undercoating used.

AES measurements revealed Cr and O and some F^- to be the main constituents of black chrome deposits, while some S and C were found only as impurities. After ion bombardment the peaks of these elements disappeared from the spectra. This is in agreement with literature data (6, 7, 11) that black chrome deposits consist of metallic chromium particles dispersed in a matrix of chromium oxides.

In order to check the thermal stability of black chrome coatings, two different types of thermal treatment have been used. In the first one black chrome specimens were heated up to 450°C for 10 h in electric furnace in an air atmosphere. In the second series, heating was done in a vacuum. From the AES spectra of thermally treated specimens, as well as from SEM investigations it has been concluded that our black chrome deposits are stable up to 350°C. Prolonged heating over this temperature especially in an air atmosphere will result in oxidation of the metallic chromium particles. After 5 h heating at 500°C no metallic chromium was found in the black chrome deposit. The heating also resulted in degradation of the selective optical response.

Figure 13A and B show the surface morphologies of black chrome deposit as defined by scanning electron mi-

Table V. Composition and experimental operating conditions for black chromium plating bath.

Compound	Concentration (g/l)
Chromic acid	420
Barium carbonate	10
Reactive 85 (NaF-citric acid-thiourea)	25
Experimental operating conditions	Black chromium plating bath
Temperature of the bath	20-25°C
Material of the anode	lead with 5% Sb
Distance anode-cathode (cm)	4
Ratio of the area anode/cathode	1

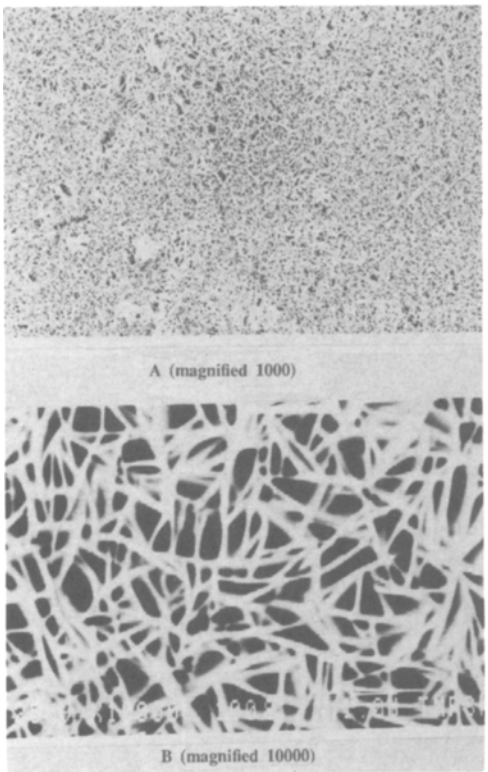

Fig. 13. SEM micrographs of black chrome deposits in "as plated" state with: A, magnification 1000 and B, magnification 10,000 times.

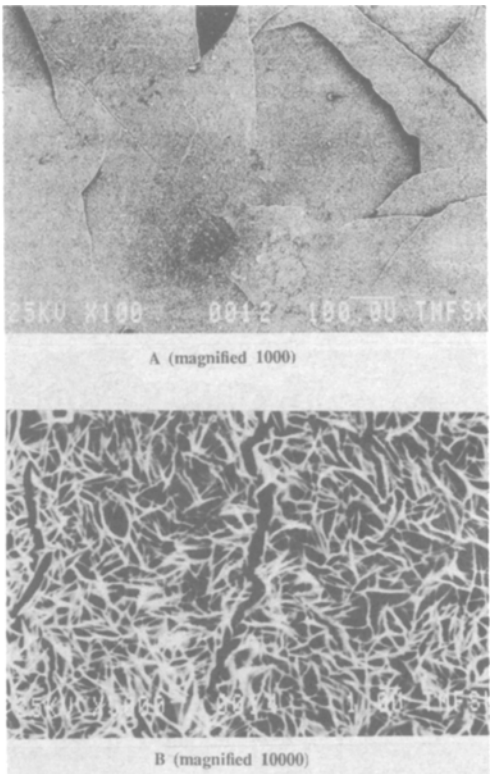

Fig. 14. SEM micrographs of black chrome deposits after thermal treatment: A, magnification 100 and B, magnification 10,000 times.

croscopy (SEM). SEM micrographs of the black chrome deposits were obtained in an "as plated" state using: A, magnification of 1000 and B, 10,000 times. One observes a dendritic growth of the deposit. This is a rather different structure from the structure of black chromium coatings deposited from acetic acid baths reported in literature (6-9). Figure 14A, magnification 100, and Fig. 14B magnification 10,000, represent the structure of thermally treated specimens. According to Fig. 14A and B thermal treatment at lower temperatures (400°C) leads to formation of microcracks. Higher temperature thermal treatment results in complete structure degradation of black chrome deposits.

Conclusions

High anodic open-circuit potentials observed on Pt cathodes in pure concentrated chromic acid and in chromic acid in which NaF, and organic compounds are added indicate that platinum passivates spontaneously. The passive film formed has an important role in the reduction mechanism because it shifts the deposition of metallic chromium and chromium oxide to very high overvoltages.

A low hydrogen overvoltage (−0.25 V *vs.* SCE) is present at the working electrode. The measured current for the entire cathodic region corresponds to hydrogen reduction and reduction of Cr electroactive species. In the presence of NaF, thiourea, and citric acid, hydrogen evolution drops drastically. Besides the reduction peak which occurs at −0.95 V in the absence of the additives, two new peaks at −0.3 V and at −0.5 V *vs.* SCE appear in their presence. The magnitude of the peak at −0.3 V *vs.* SCE does not depend upon chromic acid concentration, and neither peak depends upon the concentration of the additives, indicating that the reduction is not controlled by the ions from the electrolyte. It has been assumed that at −0.3 V oxides which have been formed at open-circuit potential are reduced. The peak which occurs at −0.5 V *vs.* SCE can be attributed to reduction of Cr(VI) to Cr(IV). The Cr(IV) species formed at this potential are further reduced to Cr(III) at −0.95 V *vs.* SCE.

An increase of the peak current and the shift of the peak potential with an increase of the sweep rate is observed for the peak at −0.95 V indicating that Cr(III) species formed at the interface block the surface for further reduction and prevent further increase of the film thickness. At more cathodic potentials, reduction to metallic chromium occurs with a hydrogen evolution as a result of water reduction at high overvoltages.

The electrolyte given in Table V was found to be most suitable for a black chrome plating process for solar absorber tubes. The optimum plating parameters proved to be a current density of 0.35 A/cm^2 and a solution temperature of 18°C. Using the above parameters a black chromium coating has been obtained with "**a**" value of 0.94 and "**e**" values of 0.07-0.12. Both thermo-optical properties of the black chromium coating were found to depend upon the deposition time but were independent of the type of the nickel undercoating used.

Acknowledgments

We thank the United Nations and MZT Skopje Yugoslavia for financial support of this research. The authors would like to express their appreciation to Dr. Carl M. Lampert from the University of Berkeley and to Dr. Derek Lovejoy from the United Nations for their helpful discussions.

Manuscript submitted March 18, 1991; revised manuscript received Aug. 12, 1991.

Texas A&M University assisted in meeting the publication costs of this article.

REFERENCES

1. C. A. Knorr, G. Munster, and H. Feigl, *Z. Elektrochem.*, **60,** 1089 (1956).
2. R. L. Sass and S. L. Eisler, *Plating,* **41,** 497 (1955).
3. E. L. King and J. A. Neptune, *J. Am. Chem. Soc.,* **77,** 3186 (1955).
4. D. N. Usachev, *Zhur. Fiz. Khim.,* **36,** 711 (1962).
5. Z. A. Sololeva and A. T. Vagramyan, *ibid.,* **36,** 752 (1962).
6. D. Rimdzhyute, M. Mitskus, and Yu Matulis, *Lietuvos T. S. R. Mokslu Akad. Darbai, Ser. B,* **4,** 91 (1959); *Chem. Abstr.,* **54,** 1922d (1960).
7. J. P. Hoare, *This Journal,* **130,** 1475 (1983).
8. J. P. Hoare, A. H. Holden, and M. A. LaBoda, *Plating Surf. Fin.,* **67,** 42 (March 1980).
9. J. P. Hoare, *This Journal,* **130,** 1475 (1983).

10. J. P. Hoare, in "Electrodeposition Technology, Theory and Practice," L. T. Romankiw and D. R. Turner, Editors, PV 87-17, p. 233, The Electrochemical Society Softbound Proceedings Series, Pennington, NJ (1987).
11. G. Dubpernell, *Plating*, **47**, 35 (1960).
12. J. C. Saiddington and G. R. Hoey, *This Journal*, **117**, 1001 (1970).
13. J. A. Sololeva and A. T. Vagramyan, *Zh. Fiz. Khim.*, **36**, 711 (1962).
14. J. C. Saiddington and G. R. Hoey, *This Journal*, **120**, 1475 (1973).
15. H. Tabor, in "Transitions of Conference on the Use of Solar Energy, 1955," University of Arizona Press, Tucson, AZ (1958).
16. C. M. Lampert and J. Washburn, *Solar Energy Mat.*, **1-1**, 82 (1979).
17. G. B. Smith and A. Ignatiev, *ibid.*, **2**, 461 (1980).
18. C. M. Lampert, *Thin Solid Films*, **7**, 75 (1980).
19. D. Bacon and A. Ignatiev, *Solar Energy Mat.*, **9**, 3 (1983).
20. G. B. Smith, G. Zajac, and A. Ignatiev, *ibid.*, **29**, 279 (1982).
21. J. Spitz, T. van Danh, and A. Aubert, *ibid.*, **1**, 189 (1979).
22. P. M. Driver, *ibid.*, **4**, 179 (1981).
23. J. P. Hoar, *J. Phys. Chem.*, **79**, 2175 (1975).
24. P. M. Driver, R. W. Johnes, C. L. Riddeford, and R. J. Simpson, *Solar Energy*, **19**, 301 (1977).
25. C. Wyon and J. Valignat, *Solar Energy Mat.*, **11**, 435 (1985).
26. A. F. Diaz and D. Schermer, *This Journal*, **132**, 2571 (1985).
27. D.-T. Chin and H. Zhang, *Electrochim. Acta*, **31**, 299 (1986).
28. G. B. Smith, A. Ignatiev, and G. Zajac, *J. Appl. Phys.*, **51**, 8 (1980).
29. B. Popov and J. V. Ivsin, *Kem. Ind.*, **36**, 103 (1987).
30. A. V. Pamfilov and A. I. Lapushauskaya, *Ukr. Khim. J.*, **26**, 46 (1960); *Chem. Abstr.*, **55**, 8916 (1961).
31. A. T. Vagramyan and D. N. Usachev, *Zh. Priklad. Khim. Leningrad*, **32**, 1900 (1958).
32. A. T. Vagramyan and D. N. Usachev, *Chem. Abstr.*, **52**, 7905h (1958).
33. D. Rimdzhyute, M. Miskus, and Yu. Matulis, *Liet TSR Akad., Darb., Ser. B*, **4**, 91 (1959); *Chem. Abstr.*, **54**, 1922d (1960).
34. A. Ignatiev, P. O'Neill, and G. Zajac, *Solar Energy Mat.*, **1**, 69 (1979).
35. S. Srinivasan and E. Gileadi, *Electrochim. Acta*, **29**, 21 (1984).

Hydride Effect on the Kinetics of the Hydrogen Evolution Reaction on Nickel Cathodes in Alkaline Media

D. M. Soares, O. Teschke,* and I. Torriani

Instituto de Fisica, UNICAMP, 13081 Campinas, SP, Brazil

ABSTRACT

The time-dependent hydrogen evolution reaction (HER) on Ni electrodes shows a large increase in electrode overpotential with time. This is ascribed to hydride formation at active Ni cathode surfaces. Hydride formation was detected by x-ray diffraction, morphological changes at the electrode surfaces, and resulting changes in secondary electron emissivities. Nickel electrodes annealed for 2 h in an argon atmosphere at 1000°C after HER did not show x-ray lines assigned to hydride. On the other hand, hard nickel electrodes (180 HV5/30) show high overvoltages as well as hydride x-ray diffraction lines after HER. By taking the variation of the nickel electronic density of state following hydrogen sorption into account, we are able to satisfactorily explain the increase in nickel overpotential after a few hours of HER.

Nickel cathodes show marked overvoltage increase with time in alkaline electrolytes (1). The challenge is to develop methods of electrode activation which give stable performance for prolonged operating periods; therefore we need a detailed understanding of the factors contributing to electrode overvoltage. In particular, time variation effects occurring on the metal must be recognized and understood. Four possible mechanisms have been postulated by previous investigators as being responsible for the increase in cathodic overpotential, η_c, in time. (*i*) Increases in η_c are caused by a loss of electrocatalytically active material from the cathode (2, 3). (*ii*) Increases in η_c are caused by a slow reduction of nickel hydroxide to nickel, which may be a poorer evolver of hydrogen. (*iii*) Increases in η_c are caused by deposition of impurities from the electrolyte into the cathode (4). (*iv*) Increases in η_c are caused by the absorption of atomic hydrogen into the lattice of the nickel cathode (5). Time effects are recoverable, and an investigation of the recovery mechanism has yielded evidence that counterindicates mechanisms (*i*), (*ii*), and (*iii*), and supports the hydrogen absorption mechanism (6, 7).

It has been conclusively shown by volumetric measurement of desorbed hydrogen that nickel does absorb atomic hydrogen during electrolytic evolution of hydrogen gas (8-15). Nickel saturated with hydrogen from a cathodic charging has been studied previously by x-ray diffraction techniques (12). The studies show that cathodic evolution of hydrogen on nickel can produce effects similar to those caused by local lattice strains. Even though the resulting hydride is unstable, a few physical properties have been reported. X-ray diffraction studies showed that the face-centered cubic structure was retained with a lattice spacing about 5.5% larger than that of pure nickel (16). Nickel containing hydrogen can exist in one of two different hydride phases. The α-hydride is simply a solid solution of hydrogen atoms in the octahedral interstices of nickel up to a H/Ni atomic ratio of 0.03 (11, 17). Above a H/Ni atomic ratio of about 0.6, only the β-hydride phases coexist. Further, Szklarska-Smialowska (11) and Smialowski (18) have shown that the β-nickel hydride phase acts as a diffusion barrier to continued hydrogen diffusion. This supports the assertion of a complicated nickel-hydrogen interaction.

The hydrogen evolution reaction in alkaline media is assumed to proceed via well-known steps (19). Hydrogen sorption with charge transfer

$$H_2O + e^- M \rightleftarrows HM + OH^- \quad [1]$$

Hydrogen desorption with charge transfer

$$HM + H_2O + e^- M \rightleftarrows H_2M + OH^- \quad [2]$$

Hydrogen desorption by recombination without charge transfer

$$HM + HM \rightleftarrows H_2M + M \quad [3]$$

The palladium electrode, when cathodically polarized at a constant current density, i, exhibits after current interruption a characteristic overpotential η transient which decays with time t. The overall η *vs.* t transient curve is usu-

* Electrochemical Society Active Member.